ANALYTICAL AND EXPERIMENTAL DESCRIBING THE HEAT TRANSFER IN METAL QUENCHING WITH WATER SPRAYS AND JETS

Fang Y., I.Sabarimana, and Specht E. *
*Author for correspondence
Chair of Thermodynamics and Combustion,
Otto von Guericke University,
Magdeburg, 39106,
Germany,
E-mail: eckehard.specht@ovgu.de

ABSTRACT

An analytically solvable mathematical model is presented to estimate heat transfer quantities in the film boiling region of metal quenched with water sprays. The model is based on the hydrodynamics of a single droplet which is separated from the metal by a vapor film. The temperature profile within the droplet is calculated as a semi-infinite body because of the short contact time. It is validated with our own experimental results and those from literature. The influence of droplet size and velocity, spray flux, surface temperature, and the salinity level are discussed. The heat transfer in the whole boiling regime was measured for metal sheets made of inconel, nicrofer, nickel, aluminum alloy and copper. The sheets, with a size of 200 mm × 200 mm and a thickness from 2 to 4 mm, are heated above Leidenfrost temperature to study the influence of various quenching parameters.

INTRODUCTION

Spray cooling has been utilized in many industrial applications where high heat flux dissipation is demanded [1, 2]. One such application is in the metal manufacturing, in which the metal surface temperature has to be controlled precisely to preserve the microstructure. At high surface temperatures, heat is transferred through a thin vapour film which isolates the water droplet from direct contact with the metal surface. This regime is commonly designated as film boiling, in which the temperature occurring at minimum heat flux is called the Leidenfrost temperature. For very low values of $\Delta T = T_s - T_w$, single-phase forced convection dominates until isolated bubbles are formed. In the nucleate boiling regime, the vapour bubbles form columns and jets until a maximum (critical) heat flux is reached [3]. The corresponding temperature is thus called the DNB temperature.

This report is a combination of experimental and analytical results. Experimentally, temperature profiles on the metal surface were measured by using infrared thermo camera. Analytically, a mathematical model for describing the heat transfer in film boiling region was proposed. Furthermore, the results from two aspects were compared and elucidated.

NOMENCLATURE

A_m	[m^2]	Average contact area
b_{solute}	[mol/kg]	Molality
c_p	[J/kgK]	Specific heat capacity at constant pressure
d_{max}	[m]	Maximum expansion
i	[-]	Van't Hoff factor
k	[W/mK]	Thermal conductivity
K_b	[-]	Ebullioscopic constant
$\dot{m}$	[kg/m^{2}s]	Impingement density
S_{min}	[m]	Minimum thickness
t_{con}	[s]	Contact time
T	[K]	Temperature
V_0	[m^3]	Droplet volume
We	[-]	Weber number

Greek symbols

α	[W/m^{2}K]	Heat transfer coefficient
ρ	[kg/m^3]	Density
δ_v	[mm]	Vapour thickness
v	[m/s]	Droplet velocity

Subscripts

d	Droplet
Lei	Leidenfrost
Li	Liquid
max	Maximum
s	Surface
sat	Saturation
w	Water

MATHEMATICAL MODEL OF HEAT TRANSFER IN FILM BOILING

Sprays are normally characterised by the distribution of liquid droplet size and velocity. So for a general insight and a better understanding of the influences of these two parameters, a mathematical model is developed using a single droplet. When a droplet contacts the hot surface at a temperature larger than T_{Lei}, a vapour cushion is formed and a contact temperature is established. For a short contact time, the droplet can be considered as a semi-infinite thermal body. Hence, the contact temperature totally depends on the ratio of heat penetration coefficient of the metal and liquid. The heat penetration coefficient is the product of thermal conductivity (k), density (ρ) and specific heat capacity at constant pressure (c_p). Due to the fact that metal has a significantly larger value than water, the contact temperature is closer to the metal surface temperature. Since the contact temperature is considerably larger than the

boiling temperature, the water evaporates immediately. Therefore, the droplet can be considered to expand almost without friction upon the vapour film. The deformation of a droplet as a result of impact depends on the Weber number *We*. For *We* < 1, a drop is only flattened slightly before bouncing. For *We* > 80-100, a drop is destroyed, resulting in different shapes [4]. Figure 1 shows the temperature profile in a bounced droplet with maximum expansion. The droplet surface on the metal side is assumed to be at boiling temperature. This indicates that the involved heat transfer depends on the temperature gradient in the fluid.

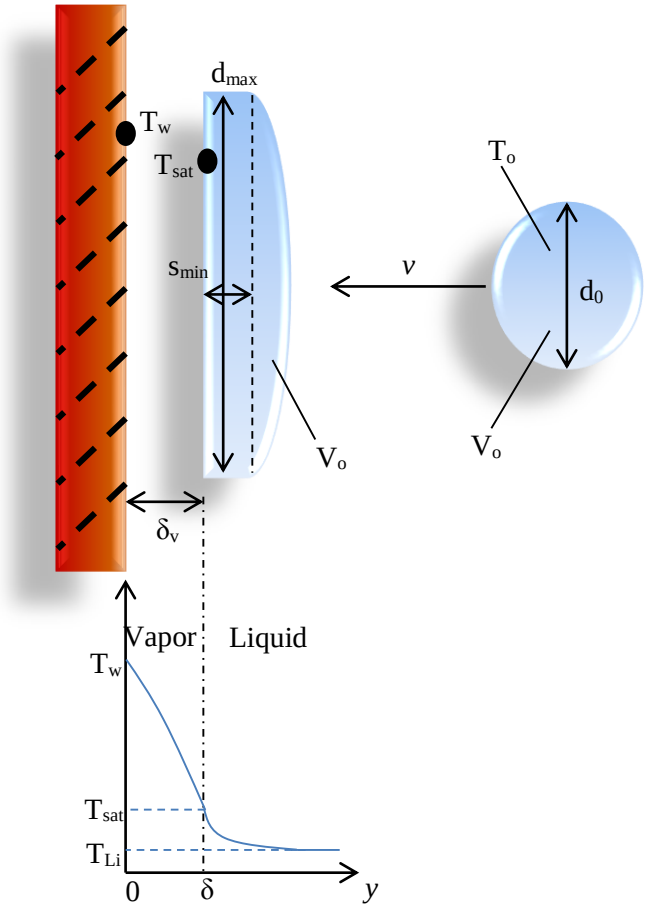

Figure 1 Schematic temperature profile of an impacting droplet above the Leidenfrost temperature

The maximum expansion of the droplet is given by the following correlation equation [5]:

$$d_{max} = 1.18d \cdot We^{0.24} = 1.18d \cdot \left(\frac{\rho \cdot v^2 \cdot d_0}{\sigma} \right)^{0.24} \quad (1)$$

where *We* is the Weber number. In this paper the droplet is considered as a disc. Due to short contact time, the volume of the droplet is assumed to be constant during the deformation. Therefore the minimum thickness can be determined. Noting that the droplet is treated as a semi-infinite body for heat conduction. This results in the calculation of heat flux into the droplet:

$$\dot{q}_d = \sqrt{\frac{(k \cdot \rho \cdot c_p)_{Li}}{\pi \cdot t_{con}}} (T_{sat} - T_{Li}) \quad (2)$$

In eq. (2), the contact time is reported by Labeish [5] to be:

$$t_{con} = 2 \cdot \frac{d}{v} \quad (3)$$

Calculations of the temperature profile in the droplet show that the opposite side does not undergo any significant change in temperature during the contact time. Then, the equation for the heat flow into the droplet is determined by:

$$Q_d = 2 \cdot \sqrt{\frac{k \cdot \rho \cdot c_p}{\pi}} \cdot (T_{sat} - T_{Li}) \cdot \sqrt{2 \frac{d_0}{v}} \cdot A_m \quad (4)$$

where A_m is the average contact area. This is assumed to be the arithmetic mean value of the maximum and minimum droplet expansion.

Furthermore, considering that the dissipated heat flux by the water spray is proportional to the number of droplets, it can be obtained by applying equations (1) to (4):

$$\dot{q} = \frac{3}{4} \cdot \sqrt{\frac{2}{\pi}} \cdot \sqrt{\frac{k \cdot \rho \cdot c_p}{\pi}} \cdot \dot{m} \cdot (T_{sat} - T_{Li}) \cdot \frac{1}{\sqrt{v \cdot d_0}} \cdot \left[1 + 1.18 \left(\frac{\rho \cdot v^2 \cdot d_0}{\sigma} \right)^{0.24} \right]^2 \quad (5)$$

Equation (5) is deduced using several assumptions. It is clear that heat flux is influenced by the impingement density, the temperature difference within the droplet, as well as the size and velocity of the droplet. It is also worth noting that equation (5) gives an implicit relation between the droplet diameter, size and the heat flux. It can be deduced that the droplet velocity is more influential than the droplet size.

The heat transfer coefficient is defined as:

$$\alpha = \frac{\dot{q}}{T_s - T_{sp}} \quad (6)$$

As heat flux is independent from the metal surface temperature T_s, the heat transfer coefficient will increase with decreasing metal surface temperature during the cooling process.

EXPERIMENTAL SETUP

Figure **2** shows the schematics of the experimental setup. It consists of four main operating units. First, an electrical furnace is used to heat up the sample. The inner temperature is adjusted, based on the sample properties, from 500°C to 850°C. Second, a cooling unit consists of a pump sucking liquid from the water tank, and a spray or jet nozzle used to generate water droplets or concentrated jets. A flow meter and a pressure gauge are mounted to control the water volume flux. A rail system is built up to facilitate the transportation of the hot metal sample from the furnace to the cooling unit. Quick movement should be guaranteed in order to avoid large heat loss. Third, there is a data acquisition system in which an infra-red (IR) camera, utilized to record temporal and spatial temperature evolution, is connected to the computer.

Before performing experiments, the metal sample needs to be prepared depending on the quenching method. For spray or single solid jet nozzles, a disc with 2 or 3 mm must be machined. After cutting, these samples are painted on one side with black furnace paint and then kept in an air-ventilated environment for around 2 hours so that the paint is dry and adhered solidly to the sample surface. The most influential step is the setting up of the

IR camera. The parameters include air humidity, ambient temperature, distance between camera lens and plate surface, surface emissivity, etc. For the purpose of the accuracy the thermal image was captured and stored at the extremely high frame rate of 150 images per second within the range of 240 × 80 pixels. The accuracy of ambient temperature measurement has the uncertainty of ±1 °C. The distance between camera lens and plate surface has an error of ±0.5 cm. The emissivity of the plate surface with black paint is measured with an uncertainty of ±0.02. After the preparation work is finished, the main cooling process follows.

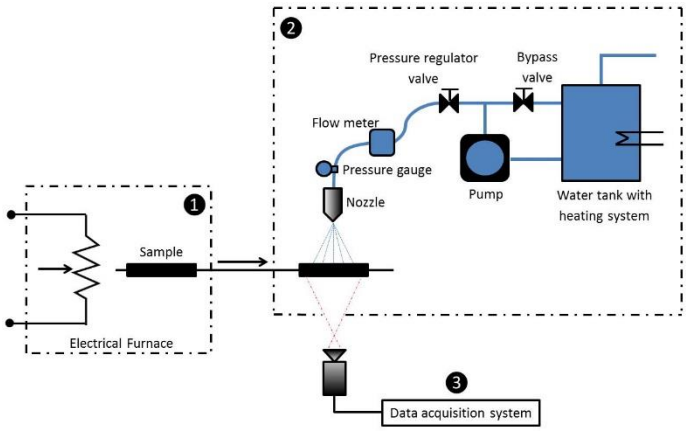

Figure 2 Diagram of quenching experiment (top view)

The impingement density was measured with a patternator, which consists of brass tubes with diameters of 10 mm by changing the distance. The impingement density can then be derived from $\dot{m} = m_d /(A\Delta t)$ where m_d is the mass of the water droplets collected, A is the area of the opening of the tube and Δt is the measurement period. The measurement was estimated to be accurate within ±4% as several repeating measurements were fluctuating in this range.

Results and discussions

In this section, the mathematical model is validated by experimental results from our own and other groups. Figure 3 shows the heat transfer coefficient in the film boiling region as a function of impingement density. The individual measured error from different authors remained in the range of 20%. Müller et al. [6] used a nickel plate with a hollow spray and a flat spray nozzle. The heat transfer coefficient increased linearly with the water impingement density. Wendelstorf et al. [3] also used nickel samples with a hydraulic nozzle. Initial temperatures were made at 600 °C and 1000 °C respectively. The same trend was observed. Al- Ahmadi et al. [7] used stainless steel samples and a hydraulic nozzle. The heat transfer coefficient is slightly lower than that of other authors. Sabariman et al. [8] used nickel plates and hydraulic spray nozzle. The achieved value lie within that of Wendelstorf et al. [3]. And results from some other authors are also included in Figure 3 [9, 10, and 11]. All mentioned authors have found no strong dependence on the size and velocity of droplets. Three correlation curves resulting from theoretical calculation of heat transfer coefficient based on equation (5) and (6) are also depicted in Figure 3. They show good agreement with the results from the experiments.

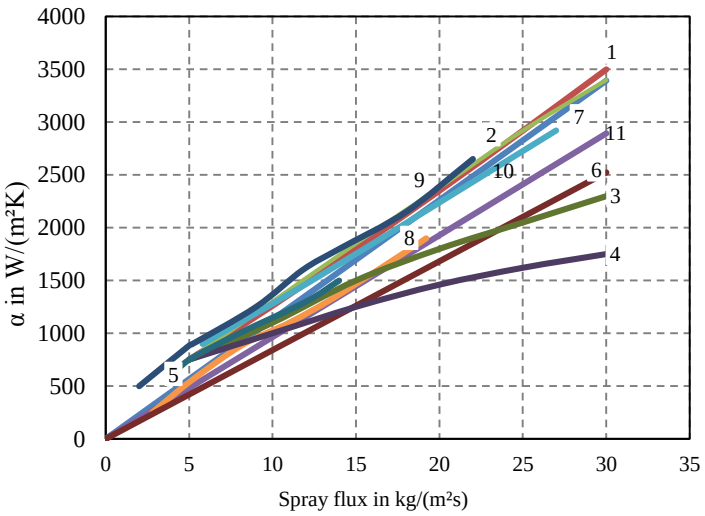

Figure 3 Comparison of experimental and theoretical study on the heat transfer coefficient versus spray flux in the film boiling region (1. Nickel at any temperature [6]; 2. Nickel at 600 °C [3]; 3. Nickel at 1000 °C [3]; 4. Steel at T_{Lei} [7]; 5. Nickel at 800 °C [8]; 6. Theory at 1000 °C (v = 30 m/s; d = 300 µm); 7. Theory at 600 °C (v = 30 m/s; d = 300 µm); 8. Steel at 700°C [9]; 9. Nickel at 600°C [10]; 10. Steel at 600°C [11]; 11. Theory at 700 °C (v = 30 m/s; d = 300 µm))

Figure 4 shows the heat transfer coefficient as a function of surface temperature in the film boiling regime. Results from different authors are included. They have used different metal materials with various impingement densities.

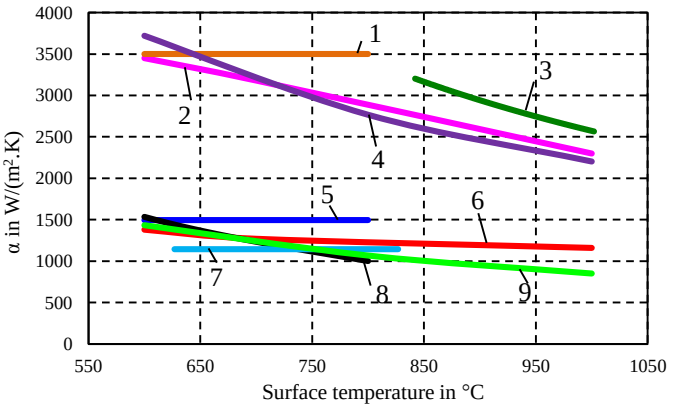

Figure 4 Comparison of experimental and theoretical study on heat transfer coefficients versus surface temperature in film boiling region (1. Nickel, 30 kg/(m²s) [6]; 2.Nickel, 30 kg/(m²s) [3]; 3. Steel, 27 kg/(m²s) [12]; 4. Theory, 30 kg/(m²s); 5. Nickel, 8 kg/(m²s) [6]; 6. Nickel, 8 kg/(m²s) [3]; 7. Steel, 6 kg/(m²s) [13]; 8. Nickel, 8 kg/(m²s) [8]; 9. Theory, 10 kg/(m²s))

Results from Müller et al. [6] show that heat transfer coefficient is independent from the surface temperature. All other results indicated that heat transfer coefficient increase with decreasing surface temperature, which comply with the theoretical calculations according to equation (5) and (6). Two

corresponding lines are also plotted in Figure 4. The results show comparable values with that obtained in experiments.

Both Figure 3 and Figure 4 show the potential of the developed mathematical model due to good agreement with the experimental results. This indicates that the model can be utilised to predict heat transfer entities qualitatively and quantitatively within a good confidence interval.

As clarified in introduction section, the Leidenfrost point characterises the beginning of transition boiling after the vapour film is destroyed. It is indicated by an abrupt heat flux increase which then reaches the maximum value within short time period. After temperature at the **d**eparture from **n**ucleate **b**oiling (DNB) point is reached, cooling proceeds in the nucleate boiling region until the surface temperature reaches the water saturation value. Because most of heat is extracted in transition and nucleate boiling, it is of great interest to investigate factors influencing the Leidenfrost and DNB temperatures.

The influence of impingement density on Leidenfrost temperature is depicted in Figure 5.

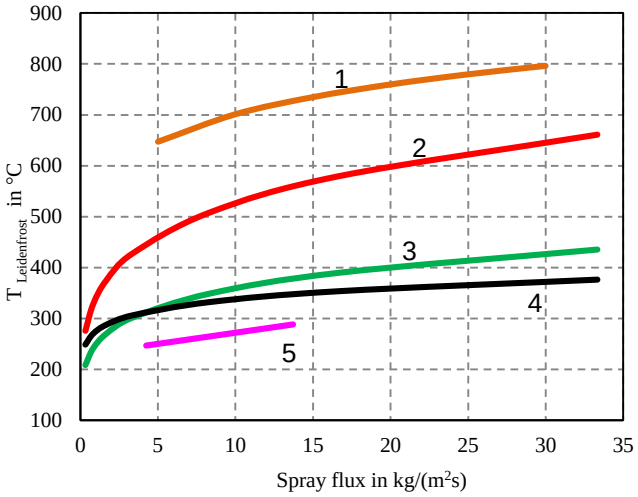

Figure 5 Leidenfrost temperature as a function of spray flux (1. Steel [7]; 2. Nickel [6]; 3. Brass M37[6]; 4. Aluminium [6]; 5. AA6082 [8])

The scatter of the results is always relatively high, which is not shown here. From the correlation it is clearly observed that less influence of spray flux on the Leidenfrost temperature occurs especially at the high level. At higher impingement densities, the influence is less strong. This indicates that a moderate spray flux should be chosen to ensure the necessary Leidenfrost point based on the purpose of the cooling process.

The salinity of water influences the heat transfer and is commonly not taken into account. However, when the liquid mass has been elevated on the vapour film, liquid on the wall side evaporates faster. This results in an increase of salt concentration on this side in the droplet. According to the model proposed by Huang et al. [14], the original concentration 0.1 M can increase to 30 M. The extent of boiling-point elevation can be calculated by applying Clausius–Clapeyron relation and Raoult's law together with the assumption of the non-volatility of the solute, which is written as followed:

$$\Delta T_b = T_{b,solution} - T_{b,pure} = K_b \cdot b_{solute} \cdot i \quad (7)$$

Based on equation (7), the boiling temperature will increase to around 130 °C. At this stage, the variations of liquid properties are no longer negligible. Dissolved ions in the water can be positively or negatively charged. Electrical conductivity (EC) is then a good measure of the ability of the material to conduct electrical current. Therefore, EC is used as an index of the total dissolved salts contained in a solution.

In this work the measured value of EC is used instead of concentration to elucidate the influence of the salinity level. Several solutions used in industrial plants during the casting process were investigated. Table 1 summarises the analysis of these solutions.

Table 1. Salts contained in the real industrial solutions

Parameters	Water	AG	BF	AF	C1
Magnesium[mg/l]	<0.03	14	<2	53	106
Calcium[mg/l]	<2	84	2	150	248.5
Sodium[mg/l]	<0.03	88	186	91	77
Sulphate[mg/l]	<5	<5	62	301	867
Carbonate[mg/l]	2.94	152.6	151	126	40.4
Chloride[mg/l]	3	11	43	195	170
EC[µS/cm]	6.7	530	841	1565	2190

In Figure 6 the trend of the Leidenfrost and DNB temperature is mapped according to the increase in EC values. It is shown that for up to 2600 µS/cm, the Leidenfrost temperature increased in the range of 10-100 °C more than that of deionized water. In addition, a higher EC value stimulates the onset of transition boiling from 165 °C for deionised water to 230 °C for the C1 solution. Compared with the effect of a single salt, both the Leidenfrost and DNB temperature of a salt mixture are similar at comparable EC values.

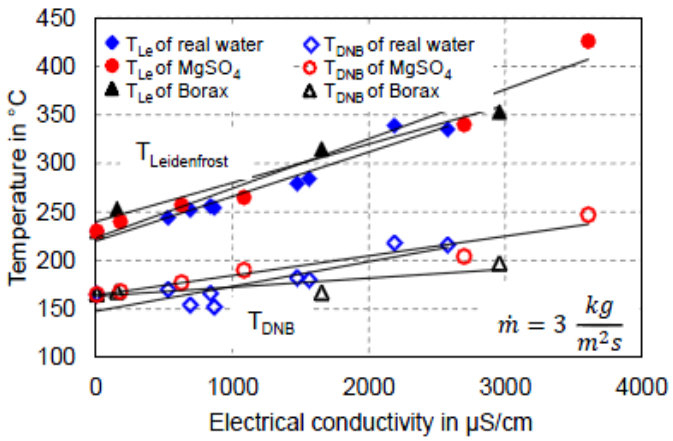

Figure 6 Leidenfrost and DNB temperature of different solutions

In order to better understand the heat transfer efficiency by a single jet nozzle, several experiments are currently under preparation. However, it is of interest to show some snapshots of wetting front propagation during the cooling process. This is shown in Figure 7. Initially the metal is heated up to 850 °C, which is indicated by bright red colour. While cooling, the metal

colour fades due to heat extraction by the single jet. Meanwhile, the water spot on the quenching surface expands towards the outside, which is depicted as dark circle in the images. In the image at 19 s, the splashed water droplet can be clearly observed due to the Leidenfrost phenomenon. Further results from these experiments may be found in future publications.

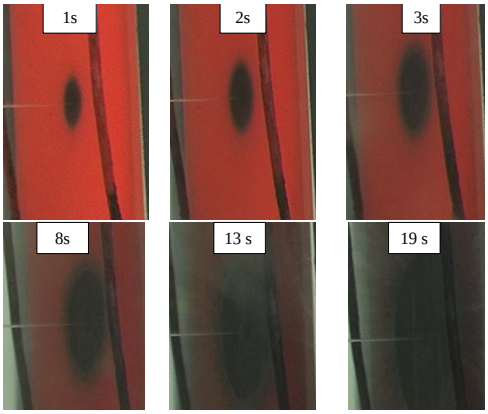

Figure 7 Snapshots during metal cooling with a solid jet nozzle

CONCLUSION

A model of single droplet in the film boiling region has been established. The influence of impingement density and surface temperature is considered as a vital parameter in the model. It is used to compare the results of homemade quenching experiments with those from other authors. A good agreement is achieved, which shows the applicability of the model. In addition, experiments are also being conducted with different qualities of water. The electrical conductivity is thus chosen as the indicator of the total dissolved salts due to the fact that it is easier to measure than the concentration. A higher EC value leads to a higher Leidenfrost and DNB temperature. This information can be utilised by industries, where the control of these two temperatures are necessary. Finally, snapshots of the experimental investigation of full jet nozzles are illustrated. They showed the expansion of the wetting front and splashed water droplet due to Leidenfrost phenomenon.

REFERENCES

[1] Mudawar, I. and Valentine, W. S., Determination of the local quench curve for spray cooled metallic surfaces, *ASM J: Heat Treating*, 1989, 7, pp. 107-121.

[2] Hall, D. D., and Mudawar, I., Experimental and numerical study of quenching complex-shaped metallic alloys with multiple, overlapping sprays, *Int. J. Heat Mass Transfer*, 1995, 38, pp. 1201-1216

[3] J. Wendelstorf, K.-H. Spitzer, R. Wendelstorf, Spray water cooling heat transfer at high temperatures and liquid mass fluxes. *Int. J. Heat Mass Transfer*, 2008, 51, pp. 4902-4910.

[4] V.G. Labeish, Thermohydrodynamic study of a drop impact against a heated wall, *Exp. Therm. Fluid Sci.*, 1994, 8, pp. 181-194.

[5] M. Nacheva, Mikromodell für den Wärmeübergang bei der Sprükülung hoch erhitzter Metalloberflächen, Fakultät für Verfahrens- und Systemtechnik, Otto-von-Guericke-Universität Magdeburg, Dissertation, 2008.

[6] H.R. Müller., and R. Jeschar, Heat transfer during water spray cooling of nonferrous metals, *Metallkunde*, 74, 1983, pp. 257-264.

[7] H.M. Al-Ahmadi and S.C. Yao, Spray cooling of high temperature metals using high mass flux industrial nozzles, *Experimental Heat Transfer*, 2008, 2, pp. 38-54.

[8] E. Specht and Sabariman, Heat transfer in spray quenching of hot metals, *Heat Processing 4*, 2014.

[9] A. Eugene, A. Mizikar, Spray cooling investigation for continuous casting of billets and blooms, Iron Steel Eng. 47 (6) (1970) 53–60.

[10] U. Reiners, Wärmeübertragung durch Spritzwasserkühlung heißer Oberflächen im Bereich der stabilen Filmverdampfung, PhD thesis, Technische Universität Clausthal, 1987.

[11] P.M. Auman, D.K. Giffiths, D.R. Hill, Hot strip mill runout table temperature control, Iron Steel Eng. (September) (1967) 174–179.

[12] J. Sanders, *Experimetelle Untersuchungen zum Wärmeübergang durch Spritzkühlung bei hohen Gießgeschwindigkeiten*, Otto-von-Guericke-Universität Magdeburg, Bachelor thesis, 2012.

[13] L. Bolle and J.C. Moureau, Spray cooling of hot surfaces, *Multiphase Science and Technology*, *Hemisphere*, 1982.

[14] C.K. Huang, and V.P. Carey, The effect of dissolved salt on the Leidenfrost transition, *Int. J. Heat Mass Transfer*, 2006, 50, pp. 269-282.